Drosophila aPKC is required for mitotic spindle orientation during symmetric division of epithelial cells

Leonardo G. Guilgur[1], Pedro Prudêncio[1], Tânia Ferreira[1], Ana Rita Pimenta-Marques[1] and Rui Gonçalo Martinho[1,2,*]

SUMMARY

Epithelial cells mostly orient the spindle along the plane of the epithelium (planar orientation) for mitosis to produce two identical daughter cells. The correct orientation of the spindle relies on the interaction between cortical polarity components and astral microtubules. Recent studies in mammalian tissue culture cells suggest that the apically localised atypical protein kinase C (aPKC) is important for the planar orientation of the mitotic spindle in dividing epithelial cells. Yet, in chicken neuroepithelial cells, aPKC is not required in vivo for spindle orientation, and it has been proposed that the polarization cues vary between different epithelial cell types and/or developmental processes. In order to investigate whether *Drosophila* aPKC is required for spindle orientation during symmetric division of epithelial cells, we took advantage of a previously isolated temperature-sensitive allele of *aPKC*. We showed that *Drosophila* aPKC is required in vivo for spindle planar orientation and apical exclusion of Pins (Raps). This suggests that the cortical cues necessary for spindle orientation are not only conserved between *Drosophila* and mammalian cells, but are also similar to those required for spindle apicobasal orientation during asymmetric cell division.

KEY WORDS: *Drosophila*, aPKC, Epithelial cells, Mitosis, Spindle orientation

INTRODUCTION

The correct orientation of the mitotic spindle is crucial for epithelial morphogenesis and the maintenance of tissue integrity (Baena-Lopez et al., 2005; Jaffe et al., 2008; Segalen and Bellaiche, 2009). Spindle orientation relies on the interaction of astral microtubules with the cell cortex and the generation of pulling forces on the attached microtubules. Cortical cues, either intrinsic or extrinsic, may determine spindle orientation through the regulation of cell polarity and cytoskeleton reorganisation (Knoblich, 2008; Siller and Doe, 2009; Yamashita and Fuller, 2008).

The molecular mechanisms driving mitotic spindle orientation have been extensively studied in the context of asymmetric cell division. *Drosophila* embryonic neuroblasts orient the mitotic spindle along the apicobasal polarity axis in order to generate two daughter cells with different sizes and cell fates (Betschinger and Knoblich, 2004; Knoblich, 2008; Siller and Doe, 2009; Yamashita and Fuller, 2008). The Par3-Par6-aPKC apical complex interacts with Inscuteable (Insc), and together they are important for spindle apicobasal orientation through the induction of apical crescents of Gαi and Pins (Raps – FlyBase) (Schaefer et al., 2001; Schaefer et al., 2000; Schober et al., 1999; Wodarz et al., 1999; Yu et al., 2003; Yu et al., 2000). Pins-like proteins and Gα subunits are key components of a highly conserved molecular machinery that links the cell cortex to the astral microtubules of the mitotic spindle (Siller and Doe, 2009).

Dividing epithelial cells mostly orient the spindle along the plane of the epithelium (planar orientation) for mitosis to produce two identical daughter cells (Jaffe et al., 2008; Segalen and Bellaiche, 2009). Although the molecular machinery that regulates mitotic spindle orientation during asymmetric cell division is well known, the identity of the cortical cues that regulate spindle orientation in symmetrically dividing epithelial cells is less understood. Recent studies in mammalian tissue culture epithelial cells suggest that, similarly to asymmetric cell divisions, the aPKC-Par6 apical complex and its positive regulator Cdc42 (Hutterer et al., 2004) are also important for planar orientation of the mitotic spindle of dividing epithelial cells (Durgan et al., 2011; Hao et al., 2010; Jaffe et al., 2008; Qin et al., 2010). Phosphorylation of LGN (the mammalian homologue of Pins; also known as Gpsm2) by apical aPKC results in the inhibition of its binding to the apically anchored Gαi and its exclusion from the apical cortical region of the dividing cell (Hao et al., 2010; Konno et al., 2008; Zheng et al., 2010). Yet, in chicken neuroepithelial cells, aPKC is not required in vivo for spindle planar orientation during symmetric cell division (Peyre et al., 2011). Since Gαi and Pins/LGN are still required for spindle planar orientation (Peyre et al., 2011) it was proposed that, whereas the molecular machinery that connects the astral microtubules to the cell cortex is conserved, the polarization cues responsible for planar orientation vary between different epithelial cell types and/or developmental processes (Peyre et al., 2011).

In order to investigate whether *Drosophila* aPKC is required for spindle planar orientation, we took advantage of a temperature-sensitive allele of *aPKC* (*apkc^{ts}*) to modulate in vivo aPKC activity. From our work we conclude that, similar to what has been reported in mammalian tissue culture cells, *Drosophila* aPKC is required for spindle planar orientation and apical exclusion of Pins during symmetric division of epithelial cells. Our observations suggest that the spindle cortical cues are conserved between *Drosophila* and mammalian cells, and we provide the first in vivo evidence for a role of aPKC in spindle planar orientation.

[1]Instituto Gulbenkian de Ciência, Rua da Quinta Grande 6, Oeiras 2781-901, Portugal. [2]Regenerative Medicine Program, Departamento de Ciências Biomédicas e Medicina, and IBB-Institute for Biotechnology and Bioengineering, Centro de Biomedicina Molecular e Estrutural, Universidade do Algarve, Campus de Gambelas, 8005-139 Faro, Portugal.

*Author for correspondence (rmartinho@igc.gulbenkian.pt)

MATERIALS AND METHODS

Fly work and genetics

Flies were raised using standard techniques. The *apkc*[ts] allele was isolated from a previously reported maternal screen (Pimenta-Marques et al., 2008). *apkc*[ts] zygotic mutant third instar larvae (L3) were obtained by crossing the *apkc*[ts]/CyO Actin-GFP stock with both the Df(2R)l4/CyO Actin-GFP and *apkc*[k06403]/CyO Actin-GFP stocks. *apkc*[ts]/Df(2R)l4 or *apkc*[ts]/apkc[k06403] larvae were selected by the absence of GFP, whereas GFP-positive larvae were used as controls. Additional control heterozygous larvae *apkc*[ts]/+, *apkc*[k06403]/+ and Df(2R)l4/+ were also used as controls for the apoptosis and spindle orientation experiments. After 24 hours egg laying at 25°C, the adults were transferred into a new vial, and the F1 progeny was shifted to 18°C, 25°C or 30°C until wing imaginal disc dissection as L3. The combination of temperatures used depended on the experiment and is indicated in each case.

For the genetic interaction between *aPKC* and *pins*, a stock was created carrying the *apkc*[ts] mutation and a strong hypomorphic allele of *pins*, *pins*[193] (Parmentier et al., 2000) (*apkc*[ts]/CyO Actin-GFP; *pins*[193]/TM6B), which was crossed with the *apkc*[k06403]/CyO Actin-GFP stock. After 24 hours egg laying at 25°C, the adults were transferred into a new vial and the F1 progeny was shifted to 28°C or 30°C. We then analysed the F1 progeny (L3 imaginal discs and adult flies) for dominant genetic interactions.

Maternal mutant embryos were obtained at 25°C from hemizygous females, *apkc*[ts]/Df(2R)l4, selected by the absence of Cy dominant marker and crossed with wild-type males.

To generate homozygous clones of *apkc*[k06403] or *apkc*[ts] that were negative for nuclear GFP label (nGFPminus), female y, w, hsFLP; FRT42B nGFP/CyO hshid flies were crossed with w; FRT42B, *apkc*[k06403]/CyO hshid or w; FRT42B, *apkc*[ts]/CyO hshid males. The offspring were heat shocked for 1 hour at 37°C at both 24 and 48 hours after a 24-hour egg collection, corresponding to the first and second larval instar. Wing discs were dissected from crawling L3 larvae, which had clones induced at first or at second instar.

Cloning of *apkc*[ts]

Complementation group 5 contained a lethal allele and a maternal sterile allele (Pimenta-Marques et al., 2008). Both alleles were mapped using the Bloomington 2R deficiency kit. Deficiencies were crossed with both alleles and F1 progeny scored for zygotic lethality and maternal sterility. The following seven deficiencies failed to complement both alleles: Df(2R)en-A, Df(2R)en-B, Df(2R)E3363, Df(2R)Exel6060, Df(2R)ix[87i3], Df(2R)ED2219 and Df(2R)ED2155; both mutant alleles mapped to the cytological interval 47E3-47F5. By a candidate gene approach we concluded that both alleles failed to complement a known lethal P-element of *aPKC* (*apkc*[k06403]).

To molecularly characterise these two potential new alleles of *aPKC*, genomic DNA was isolated from adult heterozygous flies. PCR and DNA sequencing of the *aPKC* gene locus was carried out using standard techniques. As a control for DNA polymorphisms, we used a mutant from a different complementation group isolated in the same screen. In this manuscript, we only report the molecular characterisation of the maternal sterile allele of *aPKC* (*apkc*[ts]). Although the *apkc*[ts] allele originally isolated in our screen had a second-site lethal mutation not associated with the *aPKC* gene locus and not uncovered by the Df(2R)l4 deficiency (data not shown), an *apkc*[ts] allele without this lethal mutation showed an identical temperature-sensitive viability and larval wing disc apoptosis (data not shown).

Immunohistochemistry

Third instar wing imaginal disc fixation and stainings were performed using standard procedures (Lee and Treisman, 2001). For Tubulin staining the discs were fixed in PBS containing 10% fresh formaldehyde (Sigma) and 1 mM EGTA at room temperature for 20 minutes. Wing discs were mounted in Vectashield (Vector Laboratories). For maternal phenotypic analysis, 0-6 hour embryos were fixed and stained using standard procedures (Pimenta-Marques et al., 2008) except for F-actin staining, where the vitelline membrane was removed manually. The oogenesis

phenotypic analysis was performed with tissue dissected from 2- or 3-day-old females, where mutant clones were induced by heat shock at first and second instar larval stages, and fixed in PBS containing 4% formaldehyde for 20 minutes. Embryos and ovaries were mounted in Fluorescent Mounting Medium (DakoCytomation).

Antibodies used were: rabbit anti-aPKC at 1:2000 (Santa Cruz, sc-216); mouse anti-aPKC at 1:100 (Santa Cruz, sc-17781); rabbit anti-cleaved caspase 3 at 1:500 (Cell Signaling, 9661S); mouse anti-Armadillo N2 7A1 at 1:50 [Developmental Studies Hybridoma Bank (DSHB)]; mouse anti-Neurotactin clone BP106 at 1:133 (DSHB); rat anti-DE-Cadherin at 1:20 (DCAD2, DSHB); rabbit anti-Par3 at 1:1000 (Wodarz et al., 1999); rabbit anti-pS980 Par3 at 1:50 (Morais-de-Sa et al., 2010); rabbit anti-Par6 at 1:1000 (Petronczki and Knoblich, 2001); mouse anti-pTyr at 1:1000 (Cell Signaling, 9411); rabbit anti-Lgl at 1:100 (Betschinger et al., 2003); mouse anti-Dlg clone 4F3 at 1:250 (DSHB); mouse anti-Tubulin at 1:500 (Sigma, T6199); rabbit anti-Pins at 1:1000 (Yu et al., 2000); and anti-phospho-Myosin light chain at 1:500 (Cell Signaling, 3671). For F-actin staining, a 5-minute incubation with phalloidin-Rhodamine at 1:200 (Sigma; stock concentration 1 mg/ml) was employed. For DNA staining, we used SYTOX Green (Invitrogen) at 1:5000 with 5 μg/ml RNase A in PBT (PBS+0.1% Tween-20) for 30 minutes at room temperature. Cy3- or Cy5-conjugated secondary antibodies were used at 1:1000 (Jackson ImmunoResearch, West Grove, PA, USA) and anti-rabbit Alexa Fluor 488 at 1:1000 (Molecular Probes).

Fluorescence images were obtained on a Leica TCS NT or a Zeiss LSM 510 confocal microscope. ImageJ (NIH) was used to perform measurements on transverse sections. To measure apoptosis levels the areas positive for cleaved caspase 3 were calculated (using the Freehand selection from ImageJ) and compared with a total inner ring (pouch plus hinge) average area of all discs. All measurements were performed using z-projections of larval wing discs.

Molecular biology

Drosophila RE60936 full-length *aPKC* cDNA was cloned into pDONR221 (Gateway System, Invitrogen). Site-directed mutagenesis to insert the *apkc*[ts] point mutation was performed using forward primer 5′-GTCAGCCATCCCTTCCTTAAGAATATGGATT-3′ and reverse primer 5′-AATCCATATTCTTAAGGAAGGGATGGCTGAC-3′. The wild-type and *apkc*[ts] open reading frames were fused to a UASp promoter and a 6× N-terminal Myc tag using the Gateway system (Invitrogen). Both constructs were used to generate transgenic flies (BestGene).

Western blotting

Third instar wing imaginal discs were dissected and collected. Thirty wing discs were lysed in NB buffer [50 mM Tris-Cl pH 7.5, 150 mM NaCl, 2 mM EDTA, 0.1% NP40, 1 mM DTT, 10 mM NaF and Complete Protease Inhibitor Cocktail (Roche)], protein levels were quantified (BioRad protein assay), SDS-PAGE sample buffer was added and samples were heated for 5 minutes at 100°C. Embryos at 0-6 hours after egg laying (AEL) were collected and dechorionated with 50% commercial bleach solution. Each embryonic protein sample was collected by lysing ten embryos with a needle in SDS-PAGE sample buffer and heating for 5 minutes at 100°C. Protein samples were run on 8% SDS-PAGE gels and proteins were then transferred into Hybond-ECL membranes (Amersham). Membranes were blocked overnight at 4°C in 5% non-fat milk in PBT, then primary antibodies were added to membranes and incubated overnight at 4°C. Following washes with PBT, secondary antibodies were added and incubated for 2 hours at room temperature. Protein detection was performed using ECL solution for 1 minute and Hyperfilm ECL (Amersham). Primary antibodies used were rabbit anti-aPKC at 1:2000 (Santa Cruz, sc-216) and mouse anti-alpha-Tubulin Dm1A at 1:20,000 (Sigma). Secondary detection was performed with rabbit and mouse HRP-conjugated antibodies at 1:4000 (Jackson ImmunoResearch).

Kinase assay

Embryos laid by females expressing wild-type or *apkc*[ts] Myc-tagged aPKC (aPKC[wt] and aPKC[ts]) under the control of the Actin5C-Gal4 ubiquitous driver were collected from 0 to 6 hours at 25°C. Embryos were lysed in NB buffer. Extracts were centrifuged three times at 14,000 rpm (20,817 *g*)

for 3 minutes. Owing to a consistent difference in the expression levels of Myc-tagged aPKC^{wt} and aPKC^{ts} (supplementary material Fig. S2B), different initial amounts of embryonic total protein were used to obtain comparable amounts of immunoprecipitated aPKC. As a negative control for each kinase assay, an equivalent amount of total protein from wild-type embryos (without Myc-tagged aPKC) was used for immunoprecipitation (supplementary material Fig. S2A). Protein extracts were incubated with mouse anti-Myc antibody at 1:200 (9E10, Covance) for 2 hours at 4°C. Sepharose protein G beads (Sigma) were added and incubated for 2 hours at 4°C. Beads were washed three times in NB buffer and twice with kinase buffer (250 mM HEPES pH 7.4, 0.2 mM EDTA, 1% glycerol, 150 mM NaCl, 10 mM MgCl$_2$). The kinase assay was performed by adding to the washed beads 20 µl kinase buffer supplemented with 1 µg MBP:Baz (amino acids 829-1168) [kindly provided by Daniel St Johnston (Morais-de-Sa et al., 2010)] and ATP mix [75 µM ATP and 20 µM γ^{32}P-ATP (10 Ci/mmol)] with incubation at 25°C or 30°C for 30 minutes. Samples were then heated at 100°C for 5 minutes in SDS-PAGE sample buffer. Quantification of the total levels of immunoprecipitated Myc-tagged aPKC was performed by standard western blot. To analyse aPKC kinase activity, samples were run on an SDS-PAGE gel, which was subsequently dried and analysed using a Storm 860 phosphorimager (General Electric) for quantification. The amount of MBP:Baz phosphorylation was monitored by the levels of ^{32}P incorporation, which were divided by the total amount of aPKC in order to estimate the in vitro kinase activity of aPKC. Negative controls comprised wild-type embryos immunoprecipitated with anti-Myc antibody (supplementary material Fig. S2A) or transgenic embryos carrying a Myc-tagged aPKC but where a mock immunoprecipitation was performed without adding anti-Myc antibody (Fig. 1A). Any non-specific ^{32}P incorporation observed in each negative control was subtracted from the phosphorylation detected in the respective aPKC kinase assay (Fig. 1A′,B).

Statistical analysis

Unpaired t-test was performed using Prism 5.00 for Windows (GraphPad Software, San Diego, CA, USA).

RESULTS

Isolation of a temperature-sensitive allele of *aPKC* (*apkc^{ts}*)

Previously, we isolated a collection of maternal mutants defective for early embryonic development (Pimenta-Marques et al., 2008). From this collection we identified a new allele of *atypical protein kinase C* (*apkc^{ts}*) that contained a point mutation in a highly conserved phenylalanine within the protein kinase domain (from a phenylalanine to a leucine at position 532; F532L). By comparison with the human aPKC crystal structure (Messerschmidt et al., 2005) the mutated amino acid was mapped to a hydrophobic pocket within the protein kinase domain (data not shown). Consistently, mutant Myc-tagged aPKC^{ts} immunoprecipitated from embryonic protein extracts showed a significant decrease in its in vitro kinase activity when compared with wild-type Myc-tagged aPKC^{wt} (Fig. 1A,A′).

Drosophila aPKC is an essential gene, and hemizygotes between *apkc^{k06403}* (a strong hypomorphic allele) and a deletion that uncovers the *aPKC* gene locus [Df(2R)l4] did not eclode from pupal cases (data not shown) (Rolls et al., 2003). In contrast to *apkc^{k06403}*, hemizygous mutants between *apkc^{ts}* and DF(2R)l4 or transheterozygotes between *apkc^{ts}* and *apkc^{k06403}* showed temperature-sensitive viability. Larvae hemizygous between *apkc^{ts}* and the Df(2R)l4 deletion and transheterozygous between *apkc^{ts}* and *apkc^{k06403}* were viable at 25°C (the permissive temperature), without
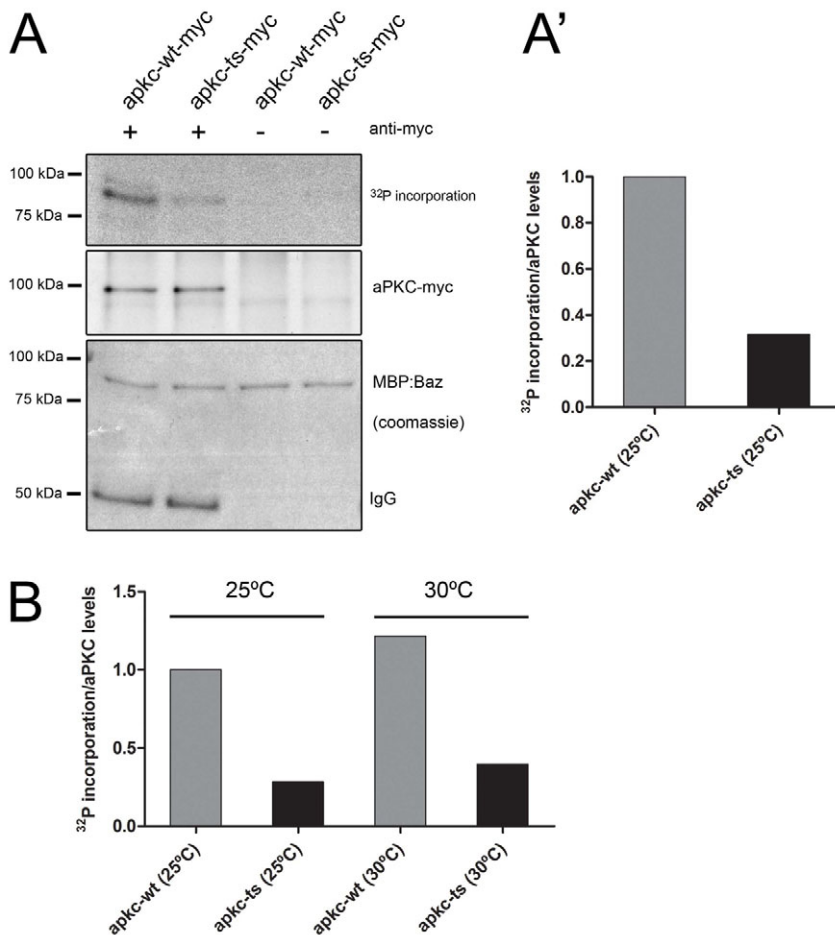

Fig. 1. aPKC^{ts} shows reduced levels of in vitro kinase activity. (**A**) Myc-tagged aPKC^{wt} and aPKC^{ts} were immunoprecipitated from *Drosophila* embryonic protein extracts and incubated with recombinant MBP:Baz (Par3) for 30 minutes at 25°C. In negative controls anti-Myc antibody was not added during immunoprecipitation. Levels of MBP:Baz phosphorylation were analysed by SDS-PAGE followed by radiography (top). Levels of MBP:Baz protein and IgGs for each assay were analysed by Coomassie Blue staining (bottom). Levels of immunoprecipitated Myc-tagged aPKC were analysed by western blot with an anti-aPKC antibody (middle). (**A′**) Relative quantification of aPKC kinase activity at 25°C (MBP:Baz phosphorylation levels/aPKC-Myc protein levels) shown in A. (**B**) Relative quantification of aPKC kinase activity at 25°C and 30°C (MBP:Baz phosphorylation levels/aPKC-Myc protein levels) shown in supplementary material Fig. S2A.

any decrease of viability (supplementary material Fig. S1A; data not shown) and adult flies were morphologically normal. By contrast, at 30°C (the restrictive temperature) most $apkc^{ts}$/Df(2R)l4 hemizygous and $apkc^{ts}$/$apkc^{k06403}$ transheterozygous larvae failed to eclode from the pupal cases, with occasional escapers flies (supplementary material Fig. S1A). At 27-28°C (semi-permissive temperature), hemizygous and transheterozygous mutant viability was highly variable (data not shown), but most adult flies showed significant abdominal midline dorsal closure defects (see below). Nevertheless, although $apkc^{ts}$ showed temperature-sensitive phenotypes, we failed to detect a decrease of $aPKC^{ts}$ in vitro kinase activity at the restrictive temperature when compared with the permissive temperature (Fig. 1B; for original kinase assay gel see supplementary material Fig. S2A).

Wing discs mutant for $apkc^{ts}$ show temperature-sensitive cell extrusion and apoptosis

In order to investigate the role of aPKC in symmetric division we took advantage of the highly proliferative larval wing disc epithelium. aPKC is essential for epithelial apicobasal polarity, the correct formation and maintenance of adherens junctions (AJs) and, consequently, for epithelial integrity (Goldstein and Macara, 2007; Knust and Bossinger, 2002; Suzuki and Ohno, 2006). Wing disc clones mutant for $apkc^{k06403}$ showed loss of epithelial integrity, cell extrusion and induction of apoptosis (Georgiou et al., 2008; Rolls et al., 2003). Consistently, we failed to detect clones mutant for $apkc^{k06403}$ (nGFP negative), in contrast to twin-spot wild-type clones (2× nGFP), if induced during first instar (supplementary material Fig. S7A,B). Moreover, the mutant clones were positive for apoptosis if induced during second instar (supplementary material Fig. S7C-F). Since the adult viability of $apkc^{ts}$ mutants was temperature sensitive, we investigated whether there was any loss of epithelial integrity at permissive and restrictive temperatures.

$apkc^{ts}$ wing discs [$apkc^{ts}$/Df(2R)l4 hemizygous or $apkc^{ts}$/$apkc^{k06403}$ transheterozygous] showed a temperature-sensitive induction of apoptosis. Whereas at the permissive temperatures (18°C and 25°C) there were low levels of cell extrusion and apoptosis (Fig. 2D,E, quantification in 2G), at the restrictive temperature (30°C) there were significantly higher levels of cell extrusion and apoptosis, and the discs were smaller than those observed in the control heterozygous larvae (Fig. 2C,F, quantification in 2G; data not shown). We failed to detect any temperature-sensitive induction of apoptosis in the control heterozygous wing discs (Fig. 2A,B, quantification in 2G). It should be noticed that the entire wing disc was mutant for $apkc^{ts}$ and we could not discern any particular pattern of apoptosis within the disc pouch (data not shown). Large clones mutant for $apkc^{ts}$ induced during first instar also showed temperature-sensitive apoptosis in L3 wing discs (supplementary material Fig. S7M-O,Y-AA). Since the wing disc epithelium mutant for $apkc^{ts}$ showed temperature-sensitive apoptosis, we concluded that it was possible to modulate the penetrance of the larval wing disc phenotypes at permissive and restrictive temperatures.

Wing discs mutant for $apkc^{ts}$ show a normal epithelial architecture even at restrictive temperature

Epithelial cells mutant for $apkc^{k06403}$ show a loss of apicobasal polarity, with an abnormal cortical distribution of AJ components and basolateral markers (Georgiou et al., 2008; Rolls et al., 2003). Since our aim was to investigate the role of aPKC in the planar orientation of the mitotic spindle, we first examined the epithelium

architecture in $apkc^{ts}$ wing discs. In order to minimize experimental artefacts, wing discs mutant for $apkc^{ts}$ [GFP negative; $apkc^{ts}$/Df(2R)l4] and control wing discs [GFP positive; $apkc^{ts}$/CyO Actin-GFP or Df(2R)l4/CyO Actin-GFP] were all pooled together for immunostaining. At restrictive temperature (30°C), the $apkc^{ts}$ epithelium was apparently normal, with normal localisation of DE-Cadherin (DE-Cad; Shotgun – FlyBase), Armadillo (Fig. 3A,B,D,E), aPKC (Fig. 3C,F) and cortical F-actin (Fig. 3I,J). We also failed to detect at restrictive temperature a significant reduction of aPKC protein levels in $apkc^{ts}$ wing discs (Fig. 2H). Moreover, the basolateral proteins Lgl [L(2)gl – FlyBase] and Dlg were efficiently excluded from the apical domain of the epithelium (Fig. 3G-J). Nevertheless, we still observed a significant amount of cell extrusion and apoptosis (cleaved caspase 3) in the basal region of $apkc^{ts}$ wing discs at the restrictive temperature (Fig. 3J).

The aPKC apical complex includes atypical protein kinase C and two PDZ-containing proteins: Par3 [Bazooka (Baz) – FlyBase] and Par6 (Par-6 – FlyBase). Par3 interacts with the aPKC-Par6 complex and is required for its apical localisation and for AJ maturation (Bilder et al., 2003; Harris and Peifer, 2005; Izumi et al., 1998; Joberty et al., 2000). In embryos, Par3 is localised slightly more basally than the aPKC-Par6 complex (Harris and Peifer, 2005). It was recently shown that aPKC-dependent phosphorylation of Par3 is required for the correct localisation of Par3 at the apical/lateral border, its exclusion from the extreme apical domain, and to regulate the interaction with the apical protein Stardust (Krahn et al., 2010; Morais-de-Sa et al., 2010). Consistent with the observation that the epithelial architecture of $apkc^{ts}$ wing discs was normal at restrictive temperature, we detected normal apical localisation of Par3 (Fig. 4A-C,E-G) and aPKC-dependent phosphorylation of Par3 (Fig. 4D,H). We conclude that, although there was a significant amount of cell extrusion and apoptosis at the restrictive temperature, the $apkc^{ts}$ epithelial cells maintained an apparently normal architecture.

aPKC is required for mitotic spindle orientation in larval wing discs

Dividing epithelial cells mostly orient the spindle along the plane of the epithelium (planar orientation). Mitotic spindle misorientation can cause a rotation of the cleavage plane of the dividing cell and an asymmetric distribution of cell junctional components between daughter cells, which may lead to epithelial cell extrusion and apoptosis. Since wing discs mutant for $apkc^{ts}$ showed at restrictive temperature a significant amount of apoptosis in an otherwise normal epithelium, we investigated whether mitotic spindle orientation was affected in dividing epithelial cells. Consistent with our hypothesis, we observed a temperature-sensitive increase in spindle misorientation in epithelial cells mutant for $apkc^{ts}$ (Fig. 5).

In control heterozygous wing discs [$apkc^{ts}$/+ and Df(2R)l4/+] the great majority of dividing cells showed (as expected) the mitotic spindle oriented along the plane of the epithelium (Fig. 5A-C, quantification in 5J; detailed statistical analysis in supplementary material Fig. S3). By contrast, in wing discs mutant for $apkc^{ts}$ [$apkc^{ts}$/Df(2R)l4 and $apkc^{ts}$/$apkc^{k06403}$] there was a significant decrease in the proportion of mitotic cells with the correct planar orientation of the spindle at permissive (Student's t-test, P=0.002) and restrictive (P=0.0001) temperatures (Fig. 5D-F,H,I, quantification in 5J; detailed statistical analysis in supplementary material Fig. S3). Importantly, and consistent with a temperature-sensitive increase in apoptosis, wing discs mutant for $apkc^{ts}$ showed a significant decrease in the proportion of mitotic cells with planar orientation of the spindle at restrictive temperature (30°C) when compared with the permissive temperature (25°C)
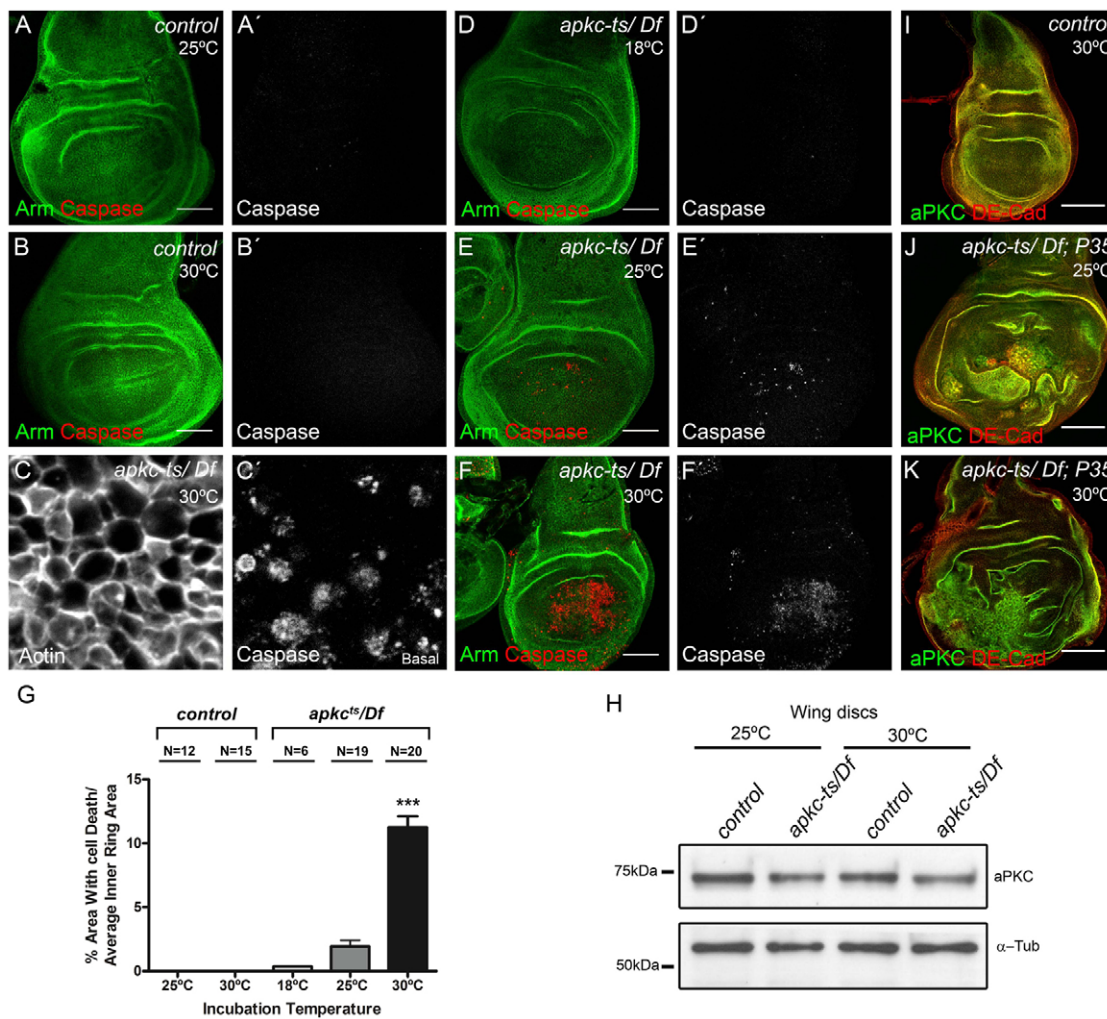
Fig. 2. *apkc^ts* mutant wing discs show temperature-sensitive apoptosis. (A-F',I-K) Third instar *Drosophila* wing imaginal discs. (**A-B'**) Control discs [heterozygous: *apkc^ts*/CyO Actin-GFP or Df(2R)l4/CyO Actin-GFP] showed absence of apoptosis at permissive (25°C, A,A') and restrictive (30°C, B,B') temperature. (**C-F'**) *apkc^ts* mutant discs [*apkc^ts*/Df(2R)l4] showed low levels of apoptosis at permissive temperatures (18°C, D,D'; 25°C, E,E'), but at restrictive temperature (30°C) they were smaller and showed high levels of apoptosis (F,F'). The apoptotic cells were mostly localised to the basal region of the mutant wing discs (C,C'). (**G**) Quantification of apoptosis levels in control and *apkc^ts* wing imaginal discs. Error bars indicate s.e.m. ***, $P<0.05$ (one-way ANOVA). (**H**) Western blot of total protein extracts of control (heterozygous) and *apkc^ts* [*apkc^ts*/Df(2R)l4] larval wing discs show similar aPKC protein levels at permissive and restrictive temperatures. (**I-K**) Inhibition of apoptosis (through the overexpression of p35) produced no obvious phenotypes in control wing discs [Scalloped-Gal4/+; *apkc^ts*/CyO Actin GFP; UAS-p35/+ or Scalloped-Gal4/+; Df(2R)l4/CyO Actin GFP; UAS-p35/+] (I). By contrast, in *apkc^ts* mutant wing discs [Scalloped-Gal4/+; *apkc^ts*/Df(2R)l4; UAS-p35/+] inhibition of apoptosis induced the development of large tumour-like tissues in the basal region of the wing disc at permissive (25°C, J) or restrictive (30°C, K) temperatures. (A-B',D-F') z projection stained for Armadillo (green) and cleaved caspase 3 (grey or red). (C,C') Standard confocal section of the basal region of the pouch respectively stained for F-actin (grey) and cleaved caspase 3 (grey). (I-K) Standard confocal sections of the basolateral region of the wing disc stained for aPKC (green) and DE-Cad (red). Scale bars: 50 μm.

(P=0.0001) (supplementary material Fig. S3). In control wing discs there was no significant difference in spindle planar orientation between permissive and restrictive temperatures (P=0.682) (Fig. 5J; supplementary material Fig. S3). We conclude that aPKC is required for the planar orientation of the mitotic spindle during the symmetric division of epithelial cells.

aPKC is required for efficient apical exclusion of Pins

In mammalian tissue culture epithelial cells, the Pins homologue LGN has to be correctly excluded from the apical cortex of the dividing cells to ensure the planar orientation of the mitotic spindle

(Konno et al., 2008; Zheng et al., 2010). Phosphorylation of LGN/Pins by apical aPKC inhibits its binding to apically anchored Gαi and thereby results in its exclusion from the apical cortical region of the dividing cell (Hao et al., 2010). Since *Drosophila* wing discs mutant for *apkc^ts* showed defects in spindle orientation, we investigated Pins localisation during mitosis.

In control wing discs, Pins cortical localisation in dividing epithelial cells (large rounded cells in Fig. 6A) was mainly basolateral when compared with DE-Cad (Fig. 6D-D''',E-E'''). At restrictive temperature, mitotic cells (large rounded cells in Fig. 6F) from *apkc^ts* discs showed a clear mislocalisation of Pins towards the epithelial apical domain as compared with DE-Cad localisation
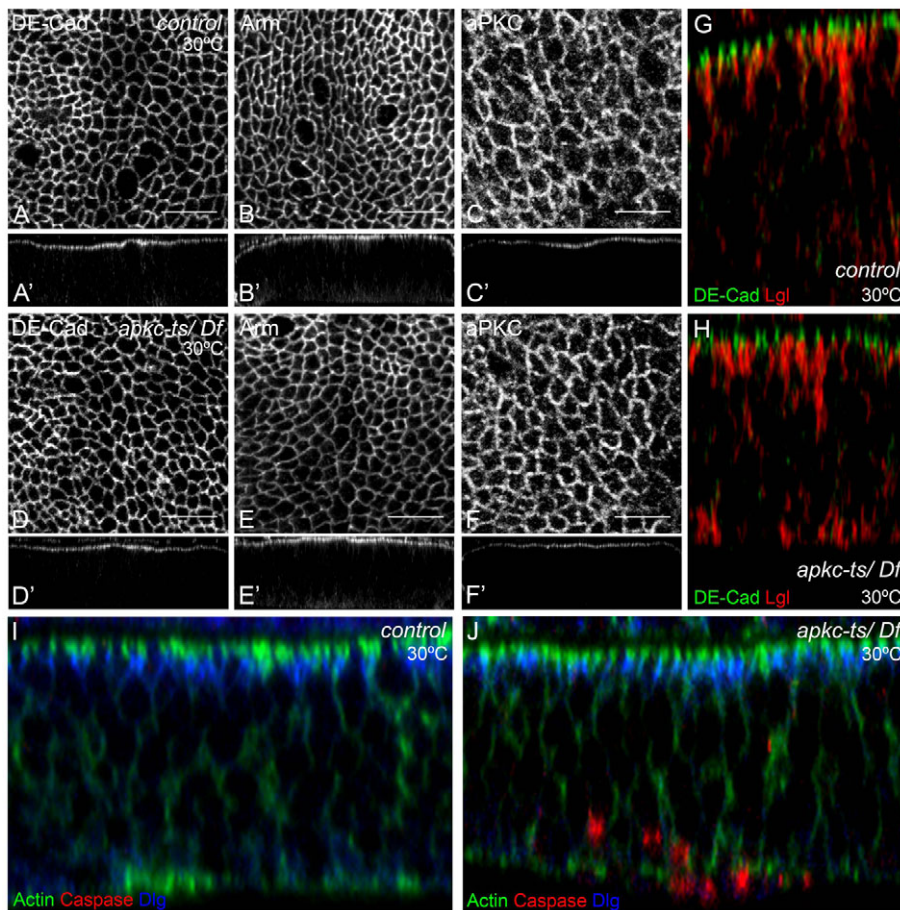
Fig. 3. Wing discs mutant for *apkc^ts* exhibit normal epithelial architecture. (**A-J**) Third instar *Drosophila* wing imaginal discs at the restrictive temperature (30°C). The *apkc^ts* [GFP negative; *apkc^ts*/Df(2R)l4] and control heterozygote [GFP positive; *apkc^ts*/CyO Actin-GFP or Df(2R)l4/CyO Actin-GFP] discs were pooled together for immunostaining. At the restrictive temperature *apkc^ts* wing discs maintained a normal epithelial architecture, with levels and localisation of adherens junction (AJ) components and apicobasal polarity markers comparable to control wing discs. (A-F) Standard confocal sections of the apical region of the pouch. (A'-F') Optical transverse sections through the pouch of wing disc epithelia stained for DE-Cad (A,A',D,D'), Armadillo (B,B',E,E') and aPKC (C,C',F,F'). (G,H,I,J) Optical transverse sections through the pouch of wing disc epithelia stained for DE-Cad (green) and Lgl (red) (G,H) or for F-actin (green), cleaved caspase 3 (red) and Dlg (blue) (I,J). Scale bars: 5 μm.

(Fig. 6G-H,I-I‴,J-J‴). The proportion of mitotic cells with apical mislocalisation of Pins in control heterozygous wing discs was zero [*n*=516 dividing cells] and in *apkc^ts*/Df(2R)l4 hemizygous wing discs was 12.75±7.97% (*n*=664) (for a breakdown of the results from four replicates see supplementary material Fig. S4).

If the apical mislocalisation of Pins was related to the *apkc^ts* wing disc phenotype, we anticipated that a reduction in *pins* expression was likely to partially suppress it. Consistently, we observed that at semi-permissive temperature, but not at restrictive temperature, a strong hypomorphic allele of *pins* [*pins^193*] (Parmentier et al., 2000)]

behaved as a dominant suppressor of *apkc^ts* wing disc apoptosis (Fig. 7A). At 28°C, *apkc^ts; pins/+* (*apkc^ts*/*apkc^k06403; pins^193*/+) wing discs showed a significant reduction (Student's *t*-test, *P*=0.0001) of apoptosis in the pouch when compared with *apkc^ts* (*apkc^ts*/*apkc^k06403*) wing discs (Fig. 7A, left). Nevertheless, such a reduction was not observed at the restrictive temperature, where the level of apoptosis was significantly higher in both mutant genotypes (Fig. 7A, right). Control discs (heterozygous: *apkc^ts*/CyO Actin-GFP or *apkc^k06403*/CyO Actin-GFP) did not show apoptosis at either temperature.
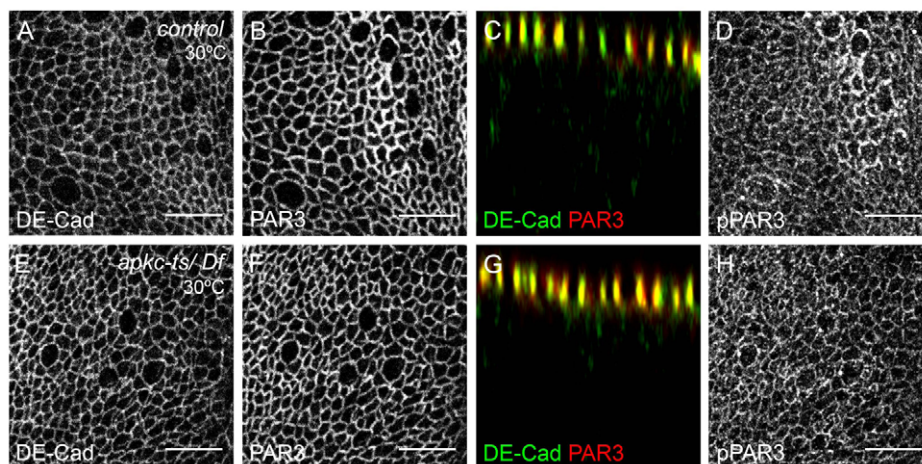

Fig. 4. Wing discs mutant for *apkc^ts* show normal apical Par3 localisation. (**A-H**) Third instar *Drosophila* wing imaginal discs at the restrictive temperature (30°C). At the restrictive temperature wing discs mutant for *apkc^ts* [*apkc^ts*/Df(2R)l4] maintained Par3 localisation at AJs and the aPKC-dependent phosphorylation of Par3 on S980 was comparable to that of control wing discs [heterozygous: *apkc^ts*/CyO Actin-GFP or Df(2R)l4/CyO Actin-GFP]. (A,B,D,E,F,H). Standard confocal sections of the apical region of the pouch stained for DE-Cad (A,E), Par3 (B,F) and phospho-S980 Par3 (D,H). (C,G) Optical transverse sections through the pouch of wing disc epithelia stained for DE-Cad (green) and Par3 (red). Scale bars: 5 μm.
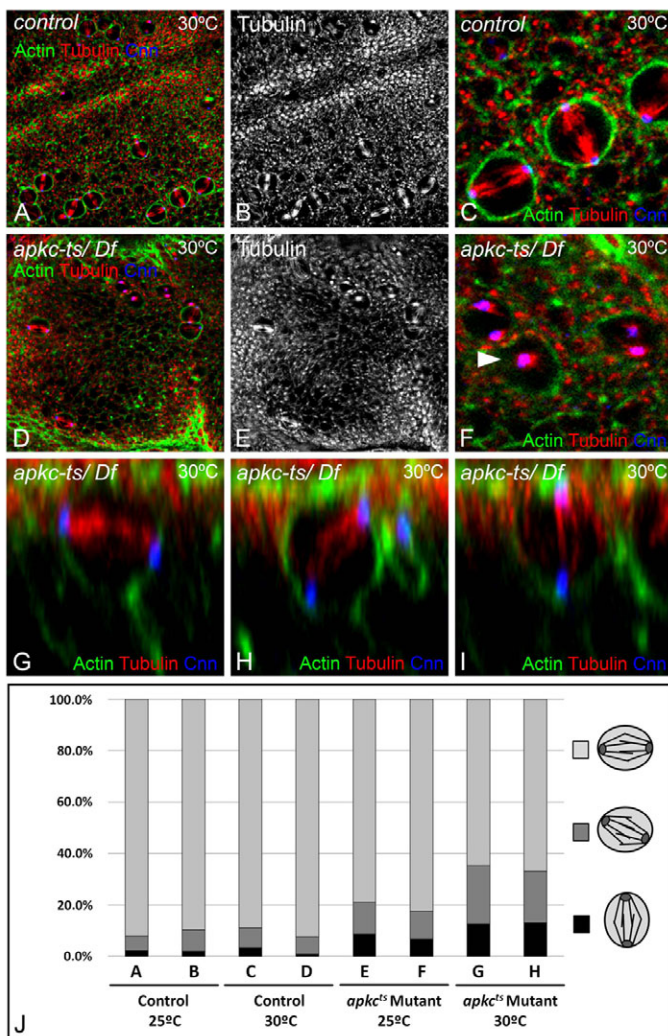
Fig. 5. aPKC is required for planar orientation of the mitotic spindle. (A-I) Third instar *Drosophila* wing imaginal discs at the restrictive temperature (30°C). (A-I) Dividing cells in control (heterozygous) wing discs mostly showed planar orientation of the mitotic spindle (A-C), whereas in *apkc^ts* [*apkc^ts*/Df(2R)l4] wing discs there was a significant increase in the frequency of spindle misorientation (D-I). The arrowhead in F points to a mitotic cell with an apicobasal orientation of the spindle. (G-I) Three images representative of the different spindle orientation categories analysed and scored in J. (J) Quantification of mitotic spindle orientation observed in control and *apkc^ts* wings discs at permissive (25°C) and restrictive (30°C) temperatures. Wing discs mutant for *apkc^ts* showed a significant decrease in the proportion of mitotic cells with planar orientation of the spindle (control 25°C versus mutant 25°C, Student's *t*-test, *P*=0.002; control 30°C versus mutant 30°C, *P*=0.0001; see also supplementary material Fig. S3). Genotypes of larval wing discs scored in J: control wing discs *apkc^ts*/+ (A,C) and Df(2R)l4/+ (B,D); *apkc^ts* mutant discs *apkc^ts*/Df(2R)l4 (E,G) and *apkc^ts*/apkc^k06403^ (F,H). Tubulin, stereotypical cell rounding and Centrosomin (Cnn) staining were used to clearly identify mitotic cells (Li and Kaufman, 1996). (A-F) Standard confocal sections of the pouch region stained for Tubulin (grey in B,E; red in A,C,D,F), F-actin (green in A,C,D,F) and Cnn (blue in A,C,D,F). (G-I) Optical transverse sections through the pouch of wing disc epithelia stained for F-actin (green), Tubulin (red) and Cnn (blue).

At the semi-permissive temperature the viability of *apkc^ts* mutants is variable (data not shown), but most adult flies show dramatic abdominal midline dorsal closure defects (Fig. 7B).

Abdominal dorsal closure defects are frequently associated with abnormalities related to histoblast proliferation and morphogenesis (Ninov et al., 2007). Interestingly, at the semi-permissive temperature *pins^193^* also behaved as a dominant suppressor, with a significant reduction in the percentage of adult flies with strong abdominal midline dorsal closure defects (from 78% in *apkc^ts* to 38% in *apkc^ts*; *pins/+*) (Fig. 7B). At the restrictive temperature, both mutant genotypes showed identical abdominal midline dorsal closure defects (Fig. 7B). Control flies did not show any abdominal defects at either temperature.

Apoptosis-induced compensatory proliferation in wing discs mutant for *apkc^ts*

Zygotic mutants of *apkc^ts* were viable and morphologically normal at the permissive temperature (supplementary material Fig. S1; data not shown), but we detected low levels of cell extrusion and apoptosis in larval wing discs (Fig. 2E,G). We hypothesized that a sublethal reduction in aPKC activity could lead to tissue overgrowth and tumour development if there were inhibition of apoptosis and compensatory cell proliferation. Consistently, at the permissive temperature inhibition of apoptosis with p35 (baculoviral caspase inhibitor protein) induced the development of large tumour-like tissues in the basal region of the larval wing discs mutant for *apkc^ts* [Scalloped-Gal4/+; *apkc^ts*/Df(2R)l4; UAS-p35/+] (Fig. 2J; supplementary material Fig. S5E,F), without affecting the apical localisation of aPKC and DE-Cad (supplementary material Fig. S5G,H). Apoptosis inhibition was not associated with the development of tumour-like tissues in the control heterozygous discs (Fig. 2I; supplementary material Fig. S5A-D).

We conclude that although viable and morphologically normal at the permissive temperature, zygotic mutants of *apkc^ts* were nevertheless extremely sensitive to apoptosis inhibition. Since inhibition of apoptosis failed to suppress the epithelial cell extrusion phenotype observed in *apkc^ts* wing discs, this suggested that apoptosis was not the cause of epithelial delamination.

Females mutant for *apkc^ts* are sterile at the permissive temperature and maternal mutant embryos show germ-band extension defects

Although viable and morphologically normal at permissive temperature, *Drosophila* females mutant for *apkc^ts* [hemizygous between *apkc^ts* and the Df(2R)l4 deletion] were nevertheless sterile, with no larvae hatching from laid eggs even when crossed with wild-type males (*n*=2428 eggs). Maternal mutant embryos for *apkc^ts* (hereafter referred to as *apkc^ts* mutant embryos) failed to complete germ-band extension (GBE), with a complete loss of epithelial integrity (supplementary material Fig. S6A-D). Similar results were obtained for maternal mutant embryos obtained from germline clones for *apkc^ts* and for maternal mutant embryos laid by females transheterozygous between *apkc^ts* and *apkc^k06403^* (data not shown). When embryos mutant for *apkc^ts* started GBE, there was a rapid delocalisation of the apically localised aPKC into cortically localised aggregates (supplementary material Fig. S6E-G). aPKC-positive aggregates were highly enriched for Par3 (supplementary material Fig. S6H-J), Par6 (supplementary material Fig. S6K,L), Armadillo and F-actin (supplementary material Fig. S6M-T). These morphogenetic defects are similar to those previously observed with a strong allele of aPKC [*apkc^k06403^* (Harris and Peifer, 2007)] (data not shown).

Yet, we detected some differences between *apkc^ts* and *apkc^k06403^*. Embryos mutant for *apkc^k06403^* (maternal mutants) showed a strong reduction in aPKC protein levels (Rolls et al., 2003), but we failed
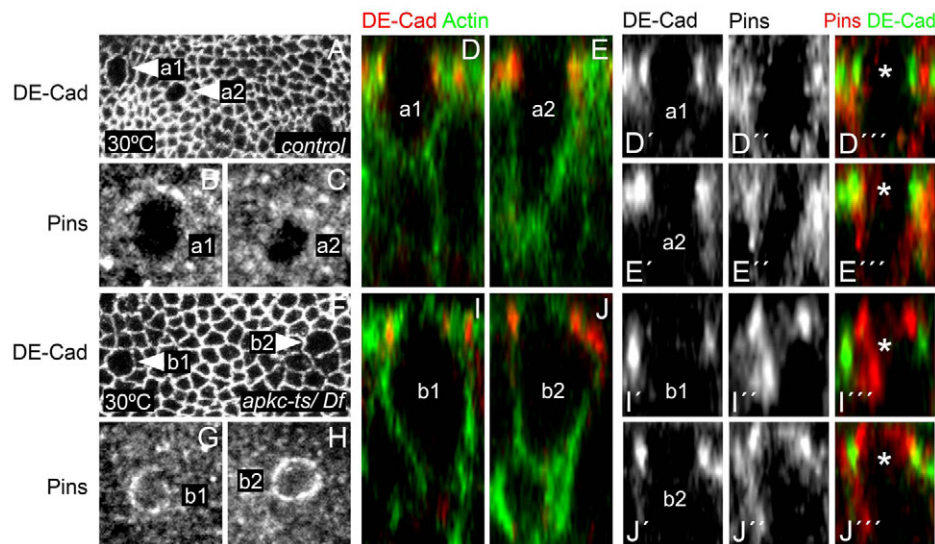
Fig. 6. aPKC is necessary for efficient apical exclusion of Pins in dividing epithelial cells. (**A-J'''**) Cells from the pouch of third instar *Drosophila* wing discs at restrictive temperature (30°C). (**A-E'''**) Mitotic cells (a1, a2, arrowheads) from the pouch of control wing discs [heterozygous: *apkc^ts*/CyO Actin-GFP or Df(2R)l4/CyO Actin-GFP] showing mainly basolateral localisation of Pins when compared with DE-Cad localisation. (**F-J'''**) By contrast, in mitotic cells (b1, b2, arrowheads) from the pouch of wing discs mutant for *apkc^ts* [*apkc^ts*/Df(2R)l4], Pins showed a clear apical enrichment when compared with DE-Cad localisation. Asterisks indicate DE-Cad position. In larval wing disc, 100% of large rounded cells (*n*=133 cells from six wing disc tissues) were mitotic (positive for Cnn), whereas 91% of mitotic cells (positive for Cnn; *n*=146 cells from six wing disc tissues) were large and showed the highly stereotypical rounded shape used to score mitosis. (A-C,F-H) Standard confocal sections of the apical region of the pouch stained for DE-Cad (grey in A,F) and Pins (grey in B,C,G,H). (D-D''',E-E''',I-I''',J-J''') Optical transverse sections through the pouch of wing disc epithelia showing the mitotic cells (a1, a2, b1,b2, as marked in A-C,F-H) stained for DE-Cad (red in D,E,I,J; grey in D',E',I',J'; green in D''',E''',I''',J'''), F-actin (green in D,E,I,J) and Pins (grey in D'',E'',I'',J''; red in D''',E''',I''',J''').

to detect such a change by western blot using *apkc^ts* embryo protein extracts (supplementary material Fig. S6X). Moreover, and similar to what was observed in larval wing discs (Fig. 3C,F; supplementary material Fig. S7G-L,S-X,AE-AJ), during blastoderm cellularisation and before the onset of GBE, we detected normal levels of apically localised aPKC in *apkc^ts* (but not *apkc^k06403*) embryos (supplementary material Fig. S6U-W), which suggested that *apkc^ts* embryos were able to apically localise aPKC but failed to correctly coordinate epithelial morphogenesis during GBE. Since the maternal phenotypes of *apkc^ts* were not temperature sensitive and were reminiscent of previously described maternal phenotypes of a strong hypomorphic allele of *aPKC* (Harris and Peifer, 2007), we concluded [in agreement with a previous suggestion (Kim et al., 2009)] that GBE was likely to require particularly high levels of aPKC activity and that epithelial tissues had differential requirements for aPKC activity during development.

Females mutant for *apkc^ts* show cyst encapsulation defects during oogenesis

At the permissive temperature (25°C) *Drosophila* females mutant for *apkc^ts* laid a significant number of eggs of normal size and shape and with correctly developed dorsal appendages (data not shown). These eggs were fertilised and the embryos developed normally until the onset of gastrulation and GBE (supplementary material Fig. S6; data not shown). Nevertheless, since at the permissive temperature females mutant for *apkc^ts* showed a reduction in egg laying compared with control heterozygous females (data not shown), we characterised oogenesis in these mutants. Somatic follicular epithelial cells mutant for *apkc^ts* showed temperature-sensitive cyst encapsulation defects after the induction of mutant clones (supplementary material Fig. S8A-D).

Interestingly, similar cyst encapsulation defects were observed at the permissive temperature (25°C) in females mutant for *apkc^ts* [hemizygous between *apkc^ts* and the Df(2R)l4 deletion or transheterozygous between *apkc^ts* and *apkc^k06403*] (supplementary material Fig. S8E-H), which suggested that the *apkc^ts* mutant phenotypes could also be modulated by allele copy number. The cyst encapsulation defects could be detected immediately after the mesenchymal-to-epithelial transition in region 3 of the germarium (supplementary material Fig. S8E), but the follicular epithelium that formed showed normal AJs (supplementary material Fig. S8E,G,H; data not shown), apicobasal polarity (supplementary material Fig. S8C,E; data not shown) and actin-myosin cytoskeleton (supplementary material Fig. S8F; data not shown).

DISCUSSION

Our study provides the first in vivo evidence for the requirement of aPKC in determining the planar orientation of the mitotic spindle during the symmetric division of epithelial cells. Furthermore, our work shows that, similar to observations in mammalian tissue culture cells, *Drosophila* aPKC is also required for the apical exclusion of Pins during mitosis. Altogether, our work suggests that the cortical cues necessary for spindle planar orientation are conserved between *Drosophila* and mammalian cells, and that they are likely to be similar to those known to be important for spindle apicobasal orientation during asymmetric cell division.

apkc^ts is a hypomorphic allele of *aPKC* with temperature-sensitive phenotypes

In this work we characterised a novel hypomorphic allele of *aPKC* (*apkc^ts*). This allele contains a point mutation at a highly conserved phenylalanine within the protein kinase domain and shows reduced
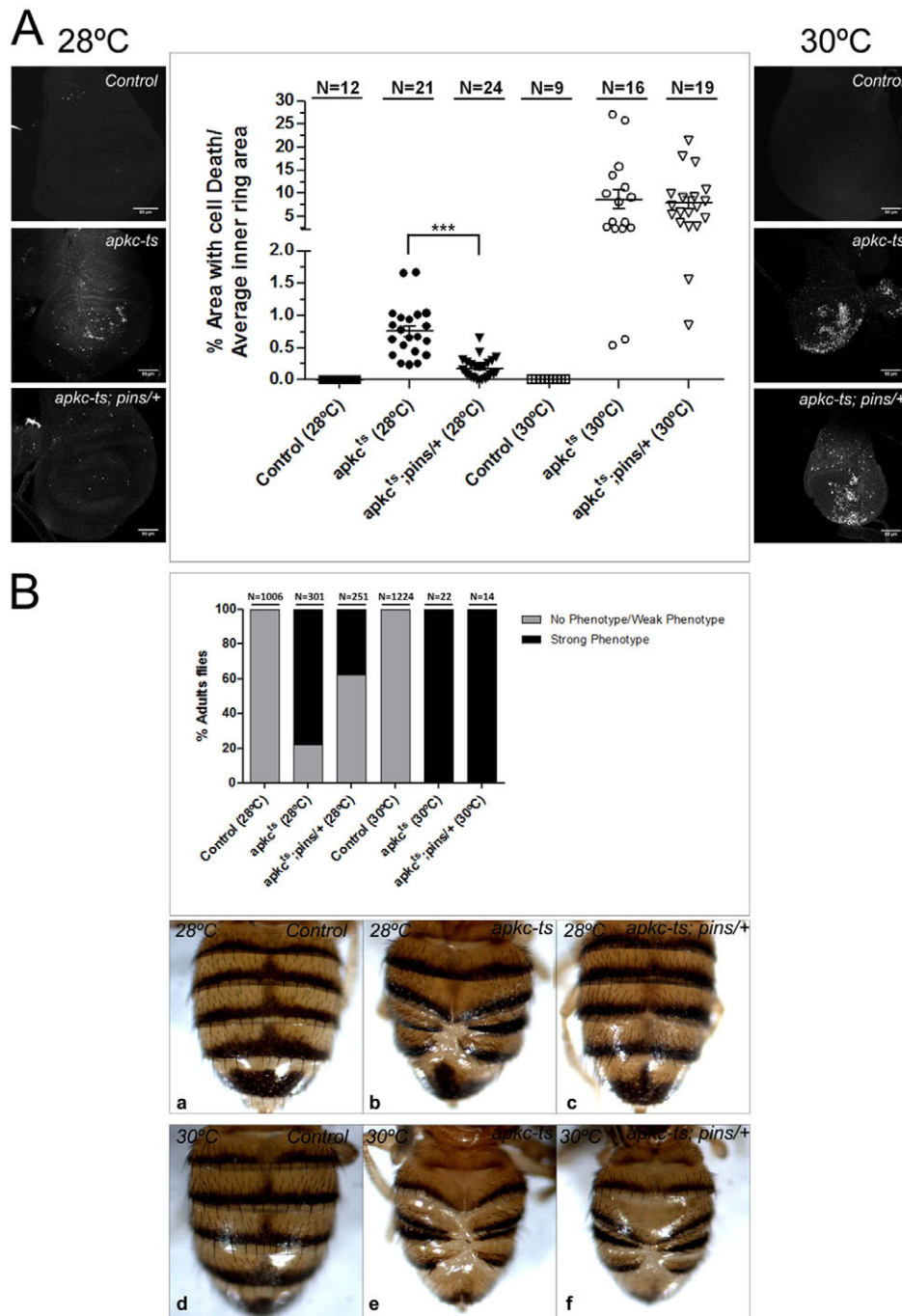
Fig. 7. A strong hypomorphic mutation of *pins* is a dominant suppressor of *apkc^ts* larval and adult phenotypes. (**A**) A strong hypomorphic mutation of *pins* (*pins^193*) behaved as a dominant suppressor of apoptosis in *apkc^ts* mutant *Drosophila* wing discs at semi-permissive temperature (28°C) but not at restrictive temperature (30°C). The centre panel shows the quantification of cleaved caspase 3 staining levels in the inner ring area of the wing discs at the different temperatures (see Materials and methods). At 28°C, *apkc^ts; pins*/+ (*apkc^ts*/*apkc^k06403*; *pins^193*/+) mutant wing discs showed a significant reduction (Student's *t*-test, *P*<0.0001) of cleaved caspase 3 staining levels in the pouch as compared with *apkc^ts* (*apkc^ts*/*apkc^k06403*) mutant discs (left). However, such reduction was not observed at 30°C (right), where the levels of caspase staining were significantly higher and similar in both mutant genotypes. Control discs (heterozygous: apkc^ts/CyO Actin-GFP or *apkc^k06403*/CyO Actin-GFP) were negative for cleaved caspase 3 at both temperatures. Left and right panels show *z* projection of wing imaginal discs stained for cleaved caspase 3 (grey). Error bars indicate s.e.m. ***, *P*<0.0001. (**B**) A strong hypomorphic mutation of *pins* behaved as a dominant suppressor of the abdominal midline dorsal closure defects at semi-permissive temperature (28°C) but not at restrictive temperature (30°C). The upper panel shows the percentage of adult flies with a strong abdominal midline dorsal closure defect (black bars) as compared with absent/weak abdominal midline phenotypes (grey bars) for each genotype at the different temperatures. At 28°C, *apkc^ts; pins*/+ mutant flies showed a significant decrease (from 78% to 38%) in the proportion of strong abdominal midline dorsal closure defects as compared with *apkc^ts* mutant flies. However, at 30°C adults flies of both mutant genotypes consistently showed similarly strong abdominal midline abdominal closure defects. Control flies did not show abdominal midline closure defects at either temperature. (**a-f**) Images representative of the different abdominal phenotype categories analysed and scored. N, number of wing discs. Scale bars: 50 µm.

levels of in vitro kinase activity without any significant reduction of aPKC protein levels or any detectable change in its apical localisation. At restrictive temperature, larval wing discs mutant for $apkc^{ts}$ showed significant levels of cell extrusion and apoptosis, yet their epithelial architecture was normal. Since loss of aPKC activity was commonly associated with a complete collapse of apicobasal polarity, abnormal AJs, apical constriction and cell extrusion, we hypothesized that the $apkc^{ts}$ allele specifically failed to complement a function of aPKC that was not directly related to apicobasal polarity and/or the formation and maintenance of junctional components. Previously, it was suggested that different epithelial tissues can have differential requirements for aPKC activity during *Drosophila* development (Kim et al., 2009). Our data expanded this hypothesis and suggested that, even within the same epithelial cell, aPKC was likely to have distinct thresholds of activity to correctly regulate different cellular processes.

Despite the fact that zygotic mutants of $apkc^{ts}$ showed significant temperature-sensitive phenotypes, we failed to detect a decrease in $aPKC^{ts}$ in vitro kinase activity at the restrictive temperature when compared with the permissive temperature. We hypothesized that the observed phenotypes were possibly due to an overhaul property of the epithelial cell whereby, at restrictive temperature, there were higher requirements for aPKC kinase activity. Alternatively, it is also possible that in vivo the $aPKC^{ts}$ mutant protein behaved as a temperature-sensitive kinase and our in vitro kinase assay failed to detect such behaviour.

Drosophila aPKC is required for mitotic spindle planar orientation

Consistent with the mammalian tissue culture work (Durgan et al., 2011; Hao et al., 2010; Qin et al., 2010), our analysis of $apkc^{ts}$ *Drosophila* wing discs revealed a requirement of aPKC for spindle orientation during symmetric mitosis. Complete randomization of spindle positioning would potentially lead to spindle misorientation in 50% of epithelial cell divisions. In $apkc^{ts}$ wing discs, there was a significant decrease in the proportion of dividing epithelial cells with the correct planar orientation of the spindle, which suggested an increase in the randomization of spindle orientation. Although it is unclear when a departure from planarity should be considered functionally significant, an increase in the randomization of spindle orientation is likely to be associated with an increase in the probability of cell extrusion and apoptosis, as misorientation of the mitotic spindle along the apicobasal axis could potentially cause rotation of the mother cell cleavage plane, a reduction of the apical and sub-apical domains of the basally localised daughter cell, and its subsequent extrusion and apoptosis. We hypothesized that spindle misorientation was likely to be one of the main causes for the cell extrusion and apoptosis phenotypes observed in $apkc^{ts}$ wing discs at restrictive temperature. Consistently, both the apoptosis and spindle orientation defects observed in the $apkc^{ts}$ wing discs were similarly temperature sensitive.

Drosophila aPKC is required for the apical exclusion of Pins

The highly conserved Pins/LGN protein is important for spindle orientation as it links the cell cortex of the dividing cell with the astral microtubules of the mitotic spindle. In mammalian epithelial tissue culture cells, LGN needs to be correctly excluded from the apical cortex of the dividing cells to ensure planar orientation of the spindle (Durgan et al., 2011; Hao et al., 2010; Jaffe et al., 2008; Konno et al., 2008; Qin et al., 2010; Zheng et al., 2010). It has been proposed that phosphorylation of LGN/Pins by apical aPKC inhibits its binding to apically anchored Gαi, resulting in its exclusion from the apical cortical region of the dividing cell (Hao et al., 2010). Consistent with this model, we observed that at restrictive temperature larval wing discs mutant for $apkc^{ts}$ showed significant mislocalisation of Pins in a subset of mitotic cells, which suggested that *Drosophila* aPKC is also required in vivo to exclude Pins from the apical domain of dividing epithelial cells.

Further supporting the hypothesis that apical mislocalisation of Pins is one of the main causes of the phenotypes observed in $apkc^{ts}$ mutants, we observed that a strong hypomorphic allele of *pins* ($pins^{193}$) could behave as a dominant suppressor of $apkc^{ts}$ wing disc apoptosis at the semi-permissive temperature. Moreover, and suggesting that the aPKC-dependent regulation of Pins is not restricted to the wing disc epithelia, we also observed that $pins^{193}$ behaved as a dominant suppressor of the abdomen dorsal closure midline defects observed in adult flies mutant for $apkc^{ts}$.

Altogether, our data suggest that aPKC is an important in vivo regulator of spindle orientation during the symmetric division of epithelial cells, with the aPKC-dependent phosphorylation of Pins resulting in its exclusion from the apical domain of dividing cells, a role that is most likely conserved between *Drosophila* and mammalian cells. Yet, and similarly to chicken neuroepithelial cells (Peyre et al., 2011), it is nevertheless possible that other *Drosophila* epithelial tissues use distinct (or possibly redundant) polarization cues [e.g. integrin signalling (Fernandez-Minan et al., 2007)] to orient the spindle during symmetric mitosis.

Our observations indicate that identical aPKC-dependent cortical cues are likely to be used to orient the mitotic spindle during symmetric and asymmetric mitosis. Similarly, Pins is required for both types of cell division, which suggests that modulation of the aPKC-dependent apical exclusion of Pins is likely to play a key role in the means by which similar cortical cues can be differentially interpreted in epithelial cells (spindle planar orientation) and neuroblasts (spindle apicobasal orientation).

Competing interests statement

The authors declare no competing financial interests.

Supplementary material

Supplementary material available online at
http://dev.biologists.org/lookup/suppl/doi:10.1242/dev.071027/-/DC1

References

Baena-Lopez, L. A., Baonza, A. and Garcia-Bellido, A. (2005). The orientation of cell divisions determines the shape of Drosophila organs. *Curr. Biol.* **15**, 1640-1644.

Betschinger, J. and Knoblich, J. A. (2004). Dare to be different: asymmetric cell division in Drosophila, C. elegans and vertebrates. *Curr. Biol.* **14**, R674-R685.

Betschinger, J., Mechtler, K. and Knoblich, J. A. (2003). The Par complex directs asymmetric cell division by phosphorylating the cytoskeletal protein Lgl. *Nature* **422**, 326-330.

Bilder, D., Schober, M. and Perrimon, N. (2003). Integrated activity of PDZ protein complexes regulates epithelial polarity. *Nat. Cell Biol.* **5**, 53-58.

Durgan, J., Kaji, N., Jin, D. and Hall, A. (2011). Par6B and Atypical PKC regulate mitotic spindle orientation during epithelial morphogenesis. *J. Biol. Chem.* **286**, 12461-12474.

Fernandez-Minan, A., Martin-Bermudo, M. D. and Gonzalez-Reyes, A. (2007). Integrin signaling regulates spindle orientation in Drosophila to preserve the follicular-epithelium monolayer. *Curr. Biol.* **17**, 683-688.

Georgiou, M., Marinari, E., Burden, J. and Baum, B. (2008). Cdc42, Par6, and aPKC regulate Arp2/3-mediated endocytosis to control local adherens junction stability. *Curr. Biol.* **18**, 1631-1638.

Goldstein, B. and Macara, I. G. (2007). The PAR proteins: fundamental players in animal cell polarization. *Dev. Cell* **13**, 609-622.

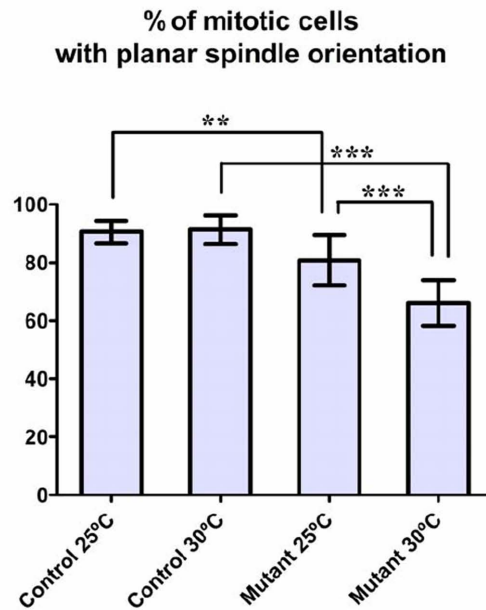Hao, Y., Du, Q., Chen, X., Zheng, Z., Balsbaugh, J. L., Maitra, S., Shabanowitz, J., Hunt, D. F. and Macara, I. G. (2010). Par3 controls epithelial spindle orientation by aPKC-mediated phosphorylation of apical pins. *Curr. Biol.* **20**, 1809-1818.

Harris, T. J. and Peifer, M. (2005). The positioning and segregation of apical cues during epithelial polarity establishment in Drosophila. *J. Cell Biol.* **170**, 813-823.

Harris, T. J. and Peifer, M. (2007). aPKC controls microtubule organization to balance adherens junction symmetry and planar polarity during development. *Dev. Cell* **12**, 727-738.

Hutterer, A., Betschinger, J., Petronczki, M. and Knoblich, J. A. (2004). Sequential roles of Cdc42, Par-6, aPKC, and Lgl in the establishment of epithelial polarity during Drosophila embryogenesis. *Dev. Cell* **6**, 845-854.

Izumi, Y., Hirose, T., Tamai, Y., Hirai, S., Nagashima, Y., Fujimoto, T., Tabuse, Y., Kemphues, K. J. and Ohno, S. (1998). An atypical PKC directly associates and colocalizes at the epithelial tight junction with ASIP, a mammalian homologue of Caenorhabditis elegans polarity protein PAR-3. *J. Cell Biol.* **143**, 95-106.

Jaffe, A. B., Kaji, N., Durgan, J. and Hall, A. (2008). Cdc42 controls spindle orientation to position the apical surface during epithelial morphogenesis. *J. Cell Biol.* **183**, 625-633.

Joberty, G., Petersen, C., Gao, L. and Macara, I. G. (2000). The cell-polarity protein Par6 links Par3 and atypical protein kinase C to Cdc42. *Nat. Cell Biol.* **2**, 531-539.

Kim, S., Gailite, I., Moussian, B., Luschnig, S., Goette, M., Fricke, K., Honemann-Capito, M., Grubmuller, H. and Wodarz, A. (2009). Kinase-activity-independent functions of atypical protein kinase C in Drosophila. *J. Cell Sci.* **122**, 3759-3771.

Knoblich, J. A. (2008). Mechanisms of asymmetric stem cell division. *Cell* **132**, 583-597.

Knust, E. and Bossinger, O. (2002). Composition and formation of intercellular junctions in epithelial cells. *Science* **298**, 1955-1959.

Konno, D., Shioi, G., Shitamukai, A., Mori, A., Kiyonari, H., Miyata, T. and Matsuzaki, F. (2008). Neuroepithelial progenitors undergo LGN-dependent planar divisions to maintain self-renewability during mammalian neurogenesis. *Nat. Cell Biol.* **10**, 93-101.

Krahn, M. P., Buckers, J., Kastrup, L. and Wodarz, A. (2010). Formation of a Bazooka-Stardust complex is essential for plasma membrane polarity in epithelia. *J. Cell Biol.* **190**, 751-760.

Lee, J. D. and Treisman, J. E. (2001). Sightless has homology to transmembrane acyltransferases and is required to generate active Hedgehog protein. *Curr. Biol.* **11**, 1147-1152.

Li, K. and Kaufman, T. C. (1996). The homeotic target gene centrosomin encodes an essential centrosomal component. *Cell* **85**, 585-596.

Messerschmidt, A., Macieira, S., Velarde, M., Badeker, M., Benda, C., Jestel, A., Brandstetter, H., Neuefeind, T. and Blaesse, M. (2005). Crystal structure of the catalytic domain of human atypical protein kinase C-iota reveals interaction mode of phosphorylation site in turn motif. *J. Mol. Biol.* **352**, 918-931.

Morais-de-Sa, E., Mirouse, V. and St Johnston, D. (2010). aPKC phosphorylation of Bazooka defines the apical/lateral border in Drosophila epithelial cells. *Cell* **141**, 509-523.

Ninov, N., Chiarelli, D. A. and Martin-Blanco, E. (2007). Extrinsic and intrinsic mechanisms directing epithelial cell sheet replacement during Drosophila metamorphosis. *Development* **134**, 367-379.

Parmentier, M. L., Woods, D., Greig, S., Phan, P. G., Radovic, A., Bryant, P. and O'Kane, C. J. (2000). Rapsynoid/partner of inscuteable controls asymmetric division of larval neuroblasts in Drosophila. *J. Neurosci.* **20**, RC84.

Petronczki, M. and Knoblich, J. A. (2001). DmPAR-6 directs epithelial polarity and asymmetric cell division of neuroblasts in Drosophila. *Nat. Cell Biol.* **3**, 43-49.

Peyre, E., Jaouen, F., Saadaoui, M., Haren, L., Merdes, A., Durbec, P. and Morin, X. (2011). A lateral belt of cortical LGN and NuMA guides mitotic spindle movements and planar division in neuroepithelial cells. *J. Cell Biol.* **193**, 141-154.

Pimenta-Marques, A., Tostoes, R., Marty, T., Barbosa, V., Lehmann, R. and Martinho, R. G. (2008). Differential requirements of a mitotic acetyltransferase in somatic and germ line cells. *Dev. Biol.* **323**, 197-206.

Qin, Y., Meisen, W. H., Hao, Y. and Macara, I. G. (2010). Tuba, a Cdc42 GEF, is required for polarized spindle orientation during epithelial cyst formation. *J. Cell Biol.* **189**, 661-669.

Rolls, M. M., Albertson, R., Shih, H. P., Lee, C. Y. and Doe, C. Q. (2003). Drosophila aPKC regulates cell polarity and cell proliferation in neuroblasts and epithelia. *J. Cell Biol.* **163**, 1089-1098.

Schaefer, M., Shevchenko, A. and Knoblich, J. A. (2000). A protein complex containing Inscuteable and the Galpha-binding protein Pins orients asymmetric cell divisions in Drosophila. *Curr. Biol.* **10**, 353-362.

Schaefer, M., Petronczki, M., Dorner, D., Forte, M. and Knoblich, J. A. (2001). Heterotrimeric G proteins direct two modes of asymmetric cell division in the Drosophila nervous system. *Cell* **107**, 183-194.

Schober, M., Schaefer, M. and Knoblich, J. A. (1999). Bazooka recruits Inscuteable to orient asymmetric cell divisions in Drosophila neuroblasts. *Nature* **402**, 548-551.

Segalen, M. and Bellaiche, Y. (2009). Cell division orientation and planar cell polarity pathways. *Semin. Cell Dev. Biol.* **20**, 972-977.

Siller, K. H. and Doe, C. Q. (2009). Spindle orientation during asymmetric cell division. *Nat. Cell Biol.* **11**, 365-374.

Suzuki, A. and Ohno, S. (2006). The PAR-aPKC system: lessons in polarity. *J. Cell Sci.* **119**, 979-987.

Wodarz, A., Ramrath, A., Kuchinke, U. and Knust, E. (1999). Bazooka provides an apical cue for Inscuteable localization in Drosophila neuroblasts. *Nature* **402**, 544-547.

Yamashita, Y. M. and Fuller, M. T. (2008). Asymmetric centrosome behavior and the mechanisms of stem cell division. *J. Cell Biol.* **180**, 261-266.

Yu, F., Morin, X., Cai, Y., Yang, X. and Chia, W. (2000). Analysis of partner of inscuteable, a novel player of Drosophila asymmetric divisions, reveals two distinct steps in inscuteable apical localization. *Cell* **100**, 399-409.

Yu, F., Cai, Y., Kaushik, R., Yang, X. and Chia, W. (2003). Distinct roles of Galphai and Gbeta13F subunits of the heterotrimeric G protein complex in the mediation of Drosophila neuroblast asymmetric divisions. *J. Cell Biol.* **162**, 623-633.

Zheng, Z., Zhu, H., Wan, Q., Liu, J., Xiao, Z., Siderovski, D. P. and Du, Q. (2010). LGN regulates mitotic spindle orientation during epithelial morphogenesis. *J. Cell Biol.* **189**, 275-288.

DEVELOPMENT

apkc^ts Zygotic Viability

A

	25°C				30°C				Incubation Temperature
	apkc-wt-myc	apkc-ts-myc	control (1)	control (2)	apkc-wt-myc	apkc-ts-myc	control (1)	control (2)	
anti-myc	+	+	+	+	+	+	+	+	

^{32}P incorporation

aPKC-myc

MBP:Baz (coomassie)

B

aPKC-myc

aPKC

A

% of mitotic cells with planar spindle orientation
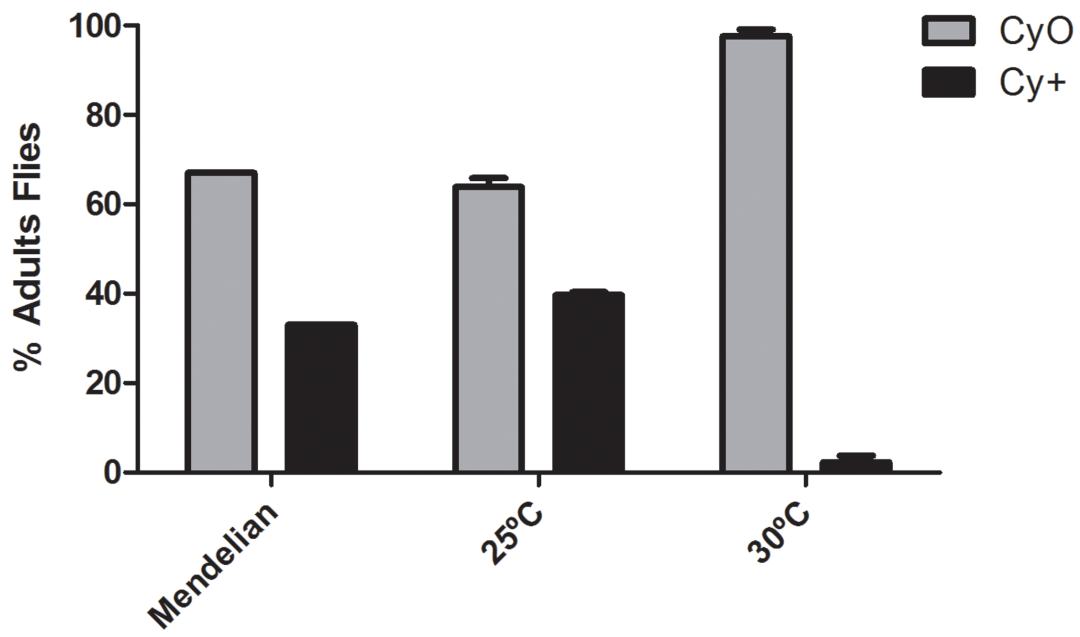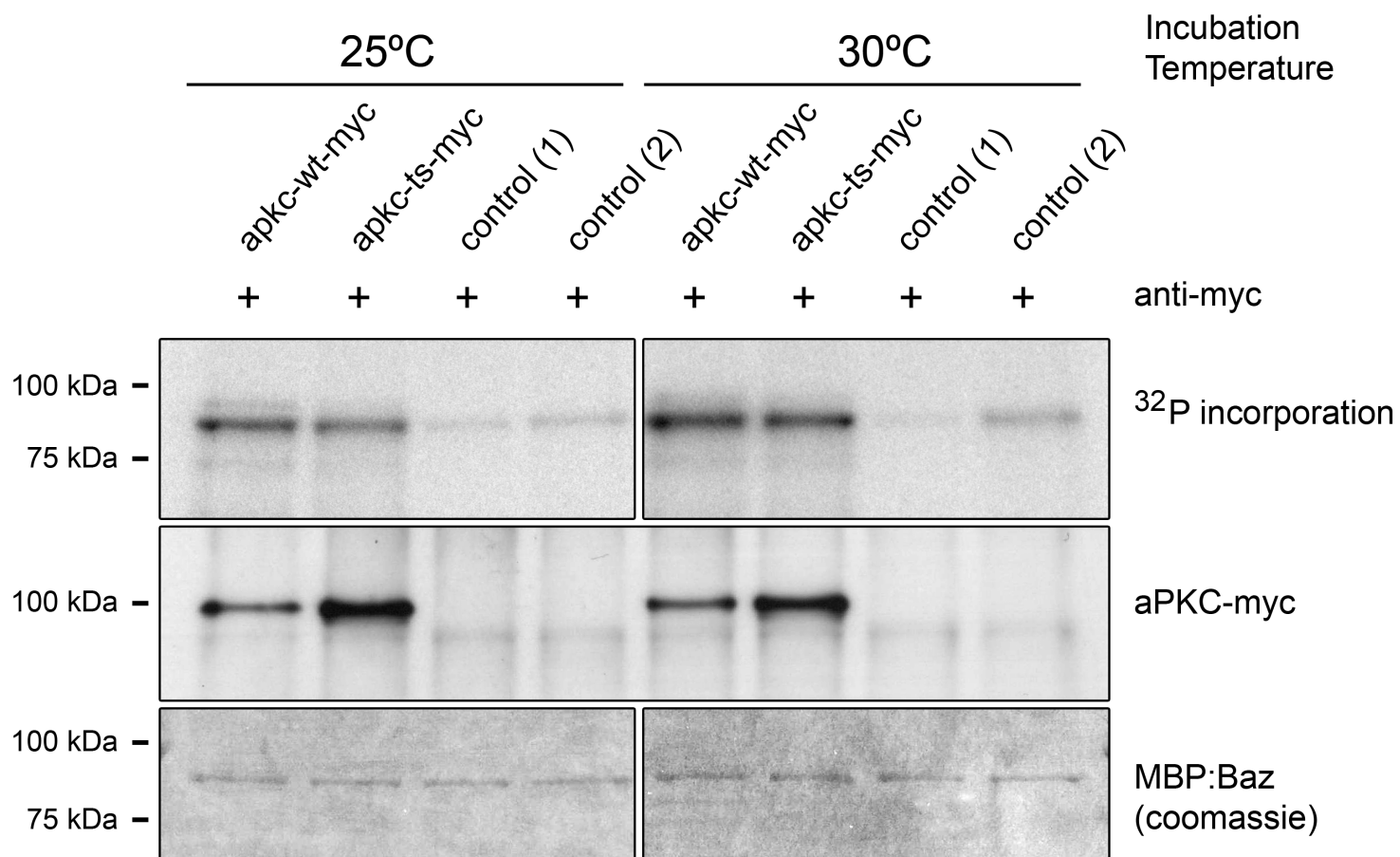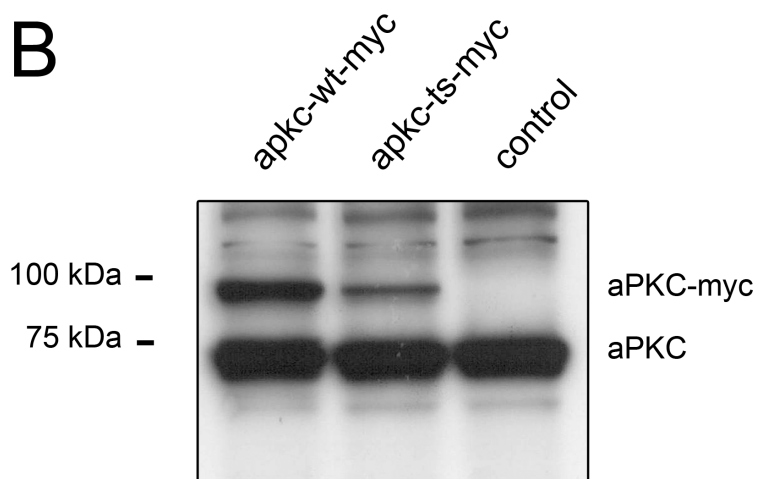
B

% of mitotic divisions with planar spindle orientation								
Genotypes compared	**Mean± SD (%)**		**≠**	**P value (t-**	**n (wing discs)**		**n (cells)**	
apkc[ts]/+(25°C) vs Df(2R)l4/+(25°C)	91.9 ± 2.03	89.4 ± 4.75	NO	P=0.281	5	6	184	192
apkc[ts]/+(30°C) vs Df(2R)l4/+(30°C)	90.0 ± 5.21	92.4 ± 4.70	NO	P=0.398	6	7	181	282
apkc[ts]/Df(2R)l4 (25°C) vs apkc[ts]/apkc[k06403](25°C)	79.7 ± 11.3	82.3± 3.11	NO	P=0.603	8	6	217	193
apkc[ts]/Df(2R)l4 (30°C) vs apkc[ts]/apkc[k06403](30°C)	65.4 ± 5.69	67.1 ± 10.2	NO	P=0.659	10	8	243	213
Control 25°C[1] vs Control 30°C[2]	90.5 ± 3.8	91.3 ± 4.8	NO	p=0.682	11	13	376	489
Control 25°C[1] vs Mutant 25°C[3]	90.5 ± 3.8	80.8 ± 8.6	YES	P=0.002	11	14	376	410
Control 25°C[1] vs Mutant 30°C[4]	90.5 ± 3.8	66.1 ± 7.8	YES	P=0.0001	11	18	376	456
Control 30°C[2] vs Mutant 25°C[3]	91.3 ± 4.8	80.8 ± 8.6	YES	P=0.0007	13	14	489	410
Control 30°C[2] vs Mutant 30°C[4]	91.3 ± 4.8	66.1 ± 7.8	YES	P=0.0001	13	18	489	456
Mutant 25°C[3] vs Mutant 30°C[4]	80.8 ± 8.6	66.1 ± 7.8	YES	P=0.0001	14	18	410	456

[1] The genotypes apkc[ts]/+ and Df(2R)l4/+ at 25ºC were pooled.
[2] The genotypes apkc[ts]/+ and Df(2R)l4/+ at 30ºC were pooled.
[3] The genotypes apkc[ts]/Df(2R)l4 and apkc[ts]/apkc[k06403] at 25ºC were pooled.
[4] The genotypes apkc[ts]/Df(2R)l4 and apkc[ts]/apkc[k06403] at 30ºC were pooled.

A control B apkc-ts C control D apkc-ts E control

DNA Nrt Nrt aPKC

F apkc-ts G apkc-ts H control I apkc-ts J apkc-ts

aPKC aPKC aPKC Par3

K control L apkc-ts M control N control O control

aPKC Par6 aPKC Actin Arm

P apkc-ts Q apkc-ts R apkc-ts S apkc-ts T apkc-ts

aPKC Actin aPKC Actin Arm

U control V apkc-ts W apkc-k06403

aPKC aPKC aPKC

X

+/+   apkc-ts GLC   apkc-ts/Df   +/Df

control band

aPKC

aPKC/Control Band

A | *apkc-k06403* clones GFP- 1st instar 25ºC | nGFP | 50 µm
B | nGFP | 20 µm
C | *apkc-k06403* clones GFP- 2nd instar 25ºC | nGFP | 50 µm
D | nGFP | 20 µm
E | Caspase | Basal
F | nGFP Caspase | 20 µm

G | *apkc-k06403* clones GFP- 2nd instar 25ºC | nGFP
H | aPKC
I | nGFP aPKC
J | *apkc-k06403* clones GFP- 2nd instar 25ºC | nGFP
K | aPKC
L | nGFP aPKC

M | *apkc-ts* clones GFP- 1st instar 25ºC | nGFP | 50 µm
N | nGFP | 20 µm
O | Caspase | Basal
P | *apkc-ts* clones GFP- 2nd instar 25ºC | nGFP | 50 µm
Q | nGFP | 20 µm
R | Caspase | Basal

S | *apkc-ts* clones GFP- 1st instar 25ºC | nGFP
T | aPKC
U | nGFP aPKC
V | *apkc-ts* clones GFP- 2nd instar 25ºC | nGFP
W | aPKC
X | nGFP aPKC

Y | *apkc-ts* clones GFP- 1st instar 30ºC | nGFP | 50 µm
Z | nGFP | 20 µm
AA | Caspase | Basal
AB | *apkc-ts* clones GFP- 2nd instar 30ºC | nGFP | 50 µm
AC | nGFP | 20 µm
AD | Caspase | Basal

AE | *apkc-ts* clones GFP- 1st instar 30ºC | nGFP
AF | aPKC
AG | nGFP aPKC
AH | *apkc-ts* clones GFP- 2nd instar 30ºC | nGFP
AI | aPKC
AJ | nGFP aPKC

A *apkc-ts* clones 25°C GFP DNA

B *apkc-ts* clones 25°C GFP aPKC

C *apkc-ts clones* 30°C GFP aPKC

D *apkc-ts clones* 30°C aPKC

E *apkc-ts*/ Df 25°C DE-Cad aPKC

F *apkc-ts*/ Df 25°C pMyosin Actin

G *apkc-ts* / + 25°C DE-Cad-GFP

H *apkc-ts*/ Df 25°C DE-Cad-GFP